SCIENCE CHINA
Technological Sciences

•Article•

May 2019 Vol.62 No.5: 849–855
https://doi.org/10.1007/s11431-018-9461-x

A descriptor of "material genes": Effective atomic size in structural unit of ionic crystals

CHEN Dong, LI ShunNing, JIE JianShu, LI SiBai, ZHENG ShiSheng, WENG MouYi, YU ChangCheng, LI ShuCheng, CHEN DaJun & PAN Feng*

School of Advanced Materials, Shenzhen Graduate School, Peking University, Shenzhen 518055, China

Received November 15, 2018; accepted January 29, 2019; published online March 21, 2019

The atomic size of each element, described by the ionic radius, is one category of "material genes" and can facilitate our understanding of atomic arrangements in compounds. Most of the ionic radii currently used to measure the sizes of cations and anions in ionic crystals are derived from hard-sphere model based on the coordination numbers, or the soft-sphere model incorporating the effect of ionic polarization. Herein we take a first step towards a novel "effective atomic size" (EAS) model, which takes into consideration the impact of the types and number of neighboring atoms on the relationship between ionic radii and interatomic distances. Taking the binary compounds between Group IA/IIA and VIA/VIIA elements gathered from the latest databases as an example, we show that the proposed EAS model can yield excellent agreement between the predicted and the DFT-calculated interatomic distances, with deviation of less than 0.1 Å. A set of EAS radii for ionic crystals has been compiled and the role of coordination numbers, geometric symmetry and distortion of structural units has been examined. Thanks to its superior predictability, the EAS model can serve as a foundation to analyze the structure of newly-discovered compounds and to accelerate materials screening processes in the future works.

ionic radii, interatomic distance, effective atomic size, coordination environment, structural units

Citation: Chen D, Li S N, Jie J S, et al. A descriptor of "material genes": Effective atomic size in structural unit of ionic crystals. Sci China Tech Sci, 2019, 62: 849–855, https://doi.org/10.1007/s11431-018-9461-x

1 Introduction

The understanding of biology has been dramatically advanced over the past decades by the strategic decision to launch the Human Genome Project that develops the genetic maps of the human being. Likewise, the project of materials genome can potentially incentivize a change in materials design by defining the descriptors for a variety of features in most materials. The project of Materials Genome Engineering is mainly composed of two parts, high throughput calculations and experiments of materials, and the database for analyzing their relation to the structures and properties, which can speed up the discovery of advanced materials. With the advent of powerful theoretical algorithms and modeling methods, the gap between Materials Genes and the macroscopic properties can be bridged [1,2]. The execution of this project raises questions about whether there are and what are the genes of a functional material. We strongly believe that the key factors lying behind material genes are associated with atomic-clusters or structure units with various elements and their arrangement of specific symmetries with different types of interatomic/molecular interaction. It seems that the first set of Material Genes ready at hand is the periodic table, which enables researchers to understand the underlying quantum mechanical mechanisms for the macroscopic chemical properties. However, it is far from realistic to precisely predict the structures and properties from the periodic table. In fact, a more feasible and common way is to

*Corresponding author (email: panfeng@pkusz.edu.cn)

define a set of descriptors that can involve quantitative data. One important category of such data is the atomic size for each element in a structure unit, as outlined by previous researchers [3–12]. Perhaps equally important is the establishment of the relationship between the atomic sizes (i.e. atomic or ionic radii) and interatomic distances in structure units of materials. Not only can such information be utilized for the investigation of possible arrangements of different atoms in a compound, but they may offer a semi-quantitative marker for the determination of defect structure [13], ionic conductivity [14], diffusion-induced stress [15], surface tension [16], and steric effects [17]. Therefore, the ability to extract a complete set of atomic radii from the materials science databases and to use them for accurate prediction of the interatomic distance, would present a significant advance in the field and help accelerate the screening and identification of novel materials. Motivated by the above considerations, we propose a novel model for atomic size in the present work to provide the project of Materials Genome a solid foundation and theoretical orientation, as a necessary step towards an efficient materials screening process in the near future.

Ever since the first attempt by Bragg [3] to assign to an atom of any element a constant radius, we have witnessed an unrelenting quest by chemists, physicists, and crystallographers alike to develop reliable methods to estimate atomic radii [4–12]. The early studies following Bragg were based on the assumption that atoms can be approximated to hard spheres and that the interatomic distance matches the sum of atomic radii of the bonded atoms. Despite the popularity of these atomic radii, from Goldschmidt's empirical [4] and Pauling's semi-theoretical [5,7,18] radii in the 1920s to the complete compilation of ionic radii proposed by Shannon et al. [11,12] four decades later, the effects of ionic polarization on the atomic sizes were totally ignored, as there was no simple way to correct the radii for polarization effects under the hard-sphere (HS) model. For Pauling's ionic radii, only the character of central element and its coordination number was considered. The HS radii can generally only apply to closed shell ionic crystals with discrepancies in interatomic distances that are outside the limits of experimental error [18,19]. Later, improvements were reached when soft-sphere (SS) model was proposed in 1978 [20]. While the HS model fails to reproduce the interatomic distances in many cases, the SS model, which treats atoms as deformable balloons or charged spheres that can overlap with each other, gives much better agreement with experiments [20–23]. The relationship between interatomic distance and SS ionic radii of an ionic crystal is given by the following equation:

$$d_{MX}{}^{k} = [M]^{k} + [X]^{k}, \quad (1)$$

where d_{MX} is the interatomic distance, $[M]$ is the radius of cation, $[X]$ is the radius of anion and the exponent k is a constant for a compound with particular structure. The value of k introduces the degree of overlap or deformation of the ions: the bigger the value of k, the larger the deformation of ions will tend to be.

The success of SS model lies in the ease with which the contribution of chemical bonding is handled in the calculations (represented by the value of k), whereas in HS model only valence state and coordination number (CN) are taken into account. Although empirical in nature, the SS model uses k as a variable to capture the degree to which the electron cloud is distorted when a chemical bond is formed [22]. Such a method can be helpful when the polarization effects are non-negligible. However, one would expect that the degree of deformation of an ion bears a strong correlation to its neighbors. For example, the degree of deformation of ions in LiCl and NaCl with sodium chloride structure should be different, as Li^{+} ion has a greater tendency than Na^{+} to withdraw the electron cloud from the Cl^{-} ion. In order to manifest such a difference, we develop an effective atomic size (EAS) model in this work. Not only the valence and coordination number of the center ion, but also the character of nearest-neighbor ions and the geometry of structural units are considered in this model. A set of EAS radii including most of the Group IA, IIA, VIA and VIIA elements is summarized, and their accuracy in reproducing the interatomic distances is verified by a sample of 148 bond length data gathered via the latest comprehensive inorganic material science databases, including material go (MG) (http://www.pkusam.com/data-base.html (accessed September 10, 2018)), materials project (MP) [24,25], inorganic crystal structure database (ICSD) [26,27] and crystallography open database (COD) [28]. Although limited to only a few elements in this work, the EAS radii proposed here should serve as a representative of a complete compilation of atomic radii corresponding to all elements in the periodic table, which will be reliable enough to predict the interatomic distances in most of the inorganic crystalline materials, and can eventually be used as descriptors to facilitate materials screening processes as a major part in the project of Materials Genome.

2 Establishment of the EAS model

In EAS model, the mathematical relationship between the ionic radii and the interatomic distance closely resembles that of SS model. The formalism of eq. (1) in SS model is based on the fact that any triangle with side lengths $[M]$, $[X]$ and d_{MX} would correspond to a specific k that makes this equation true (Figure 1(a)). Different types of compounds have different values of k: for example, k = 5/3 for alkali halides whereas k = 4/3 for alkali hydrides [22]. We note that SS model treats both cation and anion as a whole system and

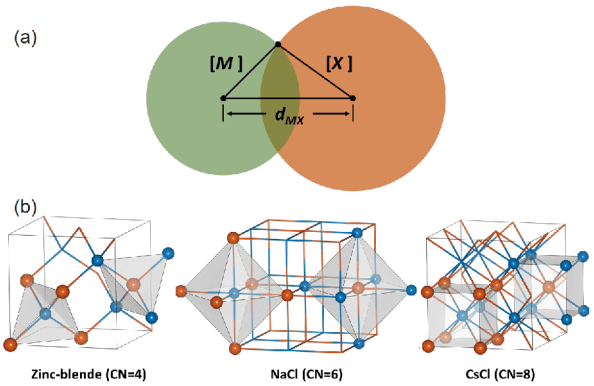

Figure 1 (Color online) (a) Interatomic distance and ionic radii of bonded ions. [*M*] is the radius of cation (green sphere), [*X*] is the radius of anion (orange sphere) and d_{MX} is interatomic distance. [*M*], [*X*] and d_{MX} form a triangle as the ions overlap with each other. (b) The structural units of zinc blende (CN=4), sodium chloride (CN=6) and cesium chloride (CN=8) structures. The orange and blue spheres represent anions and cations, respectively.

ignores the effect of neighboring atoms on the distortion of the electron cloud. Here, we separate the parameter k into two parts, k_M and k_X, corresponding to the contribution from cation and anion respectively. Therefore, the relationship between interatomic distance and the radii in EAS model follows the equation:

$$d_{MX}{}^{k_M+k_X} = [M]^{k_M+k_X} + [X]^{k_M+k_X}, \tag{2}$$

where k_M and k_X are constants for the cation and anion with particular coordination environments. Similarly, the sum of k_M and k_X represents the degree of overlap or deformation of the ions.

The approaches to derive the ionic radii are different among the HS, SS, and EAS models. In the HS model, the ionic radii are determined by the radius ratio between cation and anion, which is estimated from the effective nuclear charge [6] felt by the outer electrons [18,29]. SS model, on the other hand, first yields the radii of Na^+, Rb^+ and Cl^- ions using electron density measurements and then generates other radii using eq. (1) with an empirical value of k [22]. In this work, the set of EAS radii is formulated by fitting them, as well as k_M and k_X, to the experimental or ab initio values of interatomic distances using eq. (2). We assume that k_M and k_X can vary with different ions and their coordination environments.

The study of ionic radii for binary compounds between group IA/IIA metals and group VIA/VIIA nonmetals has long been a central concern in chemistry [11,12,20–22,30,31]. As a starting point, we investigate the alkali halides and alkaline-earth chalcogenides with zinc blende, sodium chloride and cesium chloride structures. Beryllium compounds are excluded due to their predominant covalent character. The three crystal structures selected represent three different coordination environments, thus corresponding to three values of k for each cation and anion. As shown in Figure 1(b), the coordination numbers of the structural units are 4, 6 and 8, respectively, which allows us to denote the corresponding k by $k^{(4)}$, $k^{(6)}$ and $k^{(8)}$. To carry out our fitting procedure for the EAS radii and k, we shall require that the source data contain all possible alkali halides and alkaline-earth chalcogenides with the three structures. However, for some of these compounds, experimental data are beyond reach at present time, in which case we should rely on theoretical data from first-principles calculations. It is well known that first-principles calculations [32,33] using density functional theory (DFT) [34] can generally reproduce the experimental structures within an accuracy of ~2% [35–38]. In order to ensure consistency in our methodology, all the interatomic distances in the present work are obtained from DFT calculations.

In the fitting procedure, the objective function is defined as follows:

$$d_{ij}{}^{ki+kj} = [M]_i{}^{ki+kj} + [X]_j{}^{ki+kj}, \tag{3}$$

$$\Delta d = \max\left\{\left(d_{ij} - d_{\text{source}}\right)^2\right\}, \tag{4}$$

where d_{ij} is the calculated interatomic distances from EAS model; Δd is the maximum deviation of interatomic distances; d_{source} is the interatomic distance from the set of source data; $[M]_i$ and $[X]_j$ are radii of cation i and anion j, respectively; k_i and k_j denote the contribution from the two bonded ions. Here, i = Li^+, Na^+, K^+, Rb^+, Cs^+, Mg^{2+}, Ca^{2+}, Sr^{2+}, Ba^{2+}, and j = F^-, Cl^-, Br^-, I^-, O^{2-}, S^{2-}, Se^{2-}, Te^{2-}. Through the minimization of Δd in eq. (4), we can ensure that the calculated interatomic distances match well with the DFT results. In order to preserve the periodic pattern of ionic radius, we introduce a constraint in the fitting procedure: for elements in the same group of the periodic table, the higher the atomic number, the larger is the ionic radius.

Table 1 summarizes the ionic radii from HS, SS, and EAS models. $k^{(4)}$, $k^{(6)}$ and $k^{(8)}$ in the EAS model are also listed for each ion. The interatomic distances in different coordination environments are listed in Table S1. All EAS radii of the cations are at least 0.5 Å larger than HS radii, and are 0.2–0.3 Å larger than SS radii. Elements in higher periods tend to have larger differences between EAS and HS radii, a similar trend to that between SS and HS radii [22]. This trend holds for EAS radii of the anions, while their difference from the HS radii is on a relatively small scale (below 0.5 Å). It should be recapitulated that in both SS and EAS models, ions can overlap with each other, which denies any need for the ionic radii to be close to the traditionally-used HS radii. Therefore, only when these ionic radii are used in combination with specific values of k can they have a physical meaning in the analysis of a compound. Moreover, the value of k for most elements shows a descending trend against CN,

Table 1 Ionic radii (Å) from HS, SS and EAS models, and $k^{(4)}$, $k^{(6)}$ and $k^{(8)}$ in the EAS model

		HS radii	SS radii	EAS radii	$k^{(4)}$	$k^{(6)}$	$k^{(8)}$
Cation	Li^+	0.760	1.094	1.302	2.000	1.235	0.693
	Na^+	1.020	1.497	1.732	1.274	1.185	0.954
	K^+	1.380	1.971	2.261	1.235	1.180	1.142
	Rb^+	1.520	2.160	2.438	1.228	1.117	1.173
	Cs^+	1.670	2.368	2.587	1.055	0.949	1.040
	Mg^{2+}	0.720	1.282	1.564	1.999	1.374	0.957
	Ca^{2+}	1.000	1.657	1.914	1.397	1.235	1.025
	Sr^{2+}	1.180	1.861	2.124	1.280	1.165	1.012
	Ba^{2+}	1.350	2.084	2.307	1.184	0.997	0.936
Anion	F^-	1.322	1.547	1.663	2.000	1.407	1.136
	Cl^-	1.822	2.181	2.248	1.339	1.210	0.956
	Br^-	1.983	2.372	2.415	1.294	1.136	0.875
	I^-	2.241	2.668	2.641	1.109	0.982	0.744
	O^{2-}	1.400	1.452	1.664	1.883	1.323	1.116
	S^{2-}	1.840	2.053	2.245	1.395	1.171	1.016
	Se^{2-}	1.980	2.179	2.406	1.383	1.181	0.968
	Te^{2-}	2.210	2.440	2.635	1.249	1.107	0.909

i.e., $k^{(4)} > k^{(6)} > k^{(8)}$, indicating that larger deformations of cations and anions (probably stronger interaction between them) are typically associated with smaller CN of the bonded ions. The dependence of k on the CN of structural units has demonstrated the significance of coordination environments in predicting the interatomic distances from the compilation of EAS radii.

3 Examination of compounds with simple structures of high symmetry

In Figure 2, we compare the accuracy in predicting the interatomic distances in alkali halides and alkaline-earth chalcogenides by HS, SS and EAS models. The distributions of the difference between the predicted interatomic distances ($d_{\text{predicted}}$) and the DFT results (d_{DFT}) are depicted. It should be mentioned that the results for zinc blende structure in SS model are not presented (Figure 2(a)) due to the lack of k values in the literatures. Overall, an average deviation of 0.005 Å and a maximum deviation of 0.038 Å are found for the EAS model, which are considerably smaller than those for HS (0.092 and 0.308 Å) and SS (0.051 and 0.488 Å) models. The accuracy of the EAS model appears to be not affected by the coordination environments exemplified in this work. From a mathematical point of view, these findings can be easily understood since the EAS radii are indeed obtained by fitting them to reproduce the interatomic distances from DFT calculations.

While one would expect that the maximum deviation in EAS model is determined by the amount of source data, one is tempted to cast doubt on the applicability of EAS model for predicting the interatomic distances in compounds not included in the source data. To substantiate the EAS model, we have investigated alkali chalcogenides (AC) and alkaline-earth halides (AEH) with fluorite structure. As shown in the inset of Figure 3, there are two symmetrically inequivalent sites in fluorite structure, one with a CN of 4 and an identical coordination environment (tetrahedron) to that in zinc blende, and the other with a CN of 8 and an identical coordination environment (cube) to that in cesium chloride. Therefore, the fluorite structure can be considered as a combination of the structural units in zinc blende and cesium chloride structures. In this sense, we are allowed to use not only the radii but also the $k^{(4)}$ and $k^{(6)}$ in Table 1 to predict the interatomic distances in AC and AEH with fluorite structure.

The advantage of EAS model over the other two models is illustrated in Figure 3 when we use DFT results as a reference standard. The difference between the predicted and the DFT-calculated interatomic distances is plotted in Figure S1. It is found that in EAS model, the predicted interatomic distances for nearly all the compounds investigated have fallen within one tenths of an ångström of d_{DFT}, an error range that is considered acceptable for practical application [17]. Given the somewhat arbitrary nature of the formalism in EAS model, it is quite surprising that such a model can provide an excellent match to the theoretical results from DFT calculations. It could be attributed to the fact that the effect of neighboring atoms on the relationship between atomic radii and interatomic distances is taken into account in the EAS model. We can expect that further improvements can be made by replacing eq. (2) with a more rigorous

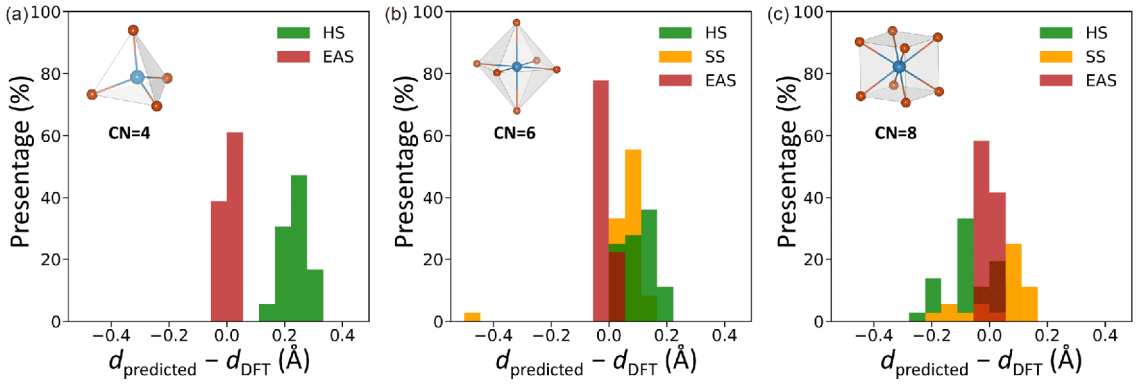

Figure 2 (Color online) The frequency distribution of the difference between the predicted interatomic distances from HS, SS and EAS models and those from DFT calculations, for alkali halides and alkaline-earth chalcogenides with (a) zinc blende structure, (b) sodium chloride structure and (c) cesium chloride structure.

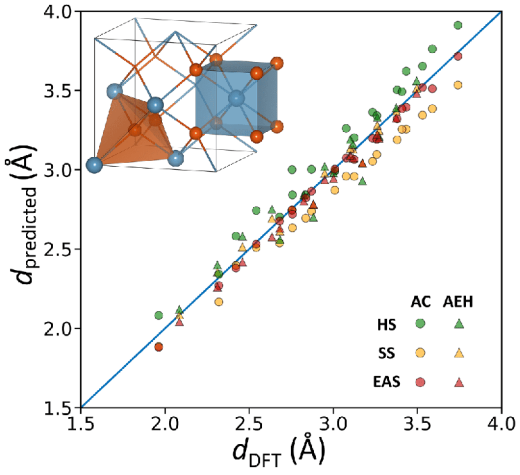

Figure 3 (Color online) Predicted interatomic distances for alkali chalcogenides and alkaline-earth halides with fluorite structure using HS, SS and EAS models, in comparison with the DFT results. The inset shows the fluorite structure and its structural units.

formalism and using a larger amount of source data, which is left for our future work.

Another feature captured in Figure 3 is that most of the interatomic distances in AC are severely underestimated by SS model, while those in AEH are close to the DFT results. This is due to the participation of several AEH compounds in obtaining the SS ionic radii [5]. Since none of the AC compounds are involved in the generation of both SS and EAS radii, we can speculate that the EAS model promises greater predictability than SS model in the analysis of completely new compounds. Nevertheless, attention must be paid when compounds with considerable covalent character are investigated in EAS model, as MgI_2, with the most covalent-like character among the AC and AEH compounds, shows the largest deviation in interatomic distance from the DFT results (0.13 Å). This discrepancy is in part due to the simplicity of the formalism in the model that yields better fit for ionic crystals.

4 Examination of compounds with distorted structural units

At this point, our next goal is to examine whether the EAS radii derived by fitting to a data set of simple structures of high symmetry can accurately describe the structural units with distortion. In order to see whether $k^{(4)}$, $k^{(6)}$ and $k^{(8)}$ can be used in compounds where structural units are distorted from perfect tetrahedron, octahedron and cube, we choose different polymorphs of MgO for preliminary consideration. There are 23 polymorphs of MgO, 5 of which are composed of MgO_4 tetrahedra connected by vertices or edges (Figure S2) while the CN of all oxygen ions is 4 as well. These facts encourage us to use $k_{Mg}^{(4)}$ and $k_O^{(6)}$ in EAS model to estimate the interatomic distances. The deviation from DFT results are all within 0.1 Å, with the highest value of 0.097 Å observed in a structure where there exist large tunnels constructed by distorted MgO_4 tetrahedra.

Similarly, we consider compounds with 6-coordinated Mg. As shown in Figure 4, two kinds of structural units (MgO_6), octahedron and triangular prism, are present in the 5 different polymorphs. Intriguingly, all the predicted interatomic distances agree well with the DFT results with a deviation of less than 0.05 Å, which indicates that the impact of geometric symmetry on k can be reasonably ignored. This can be rationalized by the fact that the electrostatic force in ionic crystals is isotropic; that is to say, the bonding strength excludes any contribution from the angular position of the nearest-neighbor atoms. In this context, the value of k still holds when the distortion of structural unit is on an acceptable scale. Our results not only validate the wide applicability of k in dealing with various structures, but also underscore the essential role of CN in selecting the value of k in the EAS model. The importance of CN has been fre-

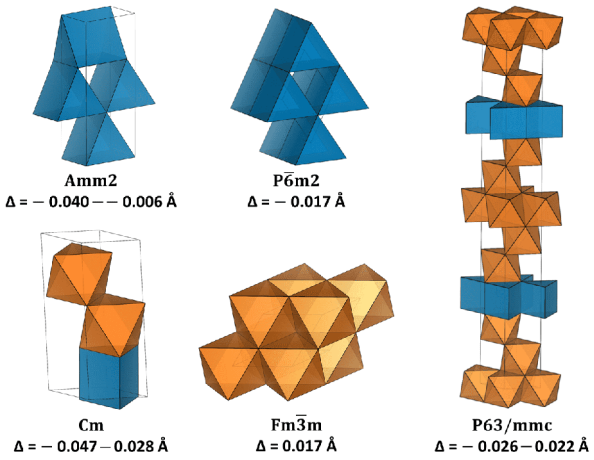

Figure 4 (Color online) The spatial arrangements of MgO_6 structural units (including octahedron and triangular prism) in 5 representative MgO polymorphs. The octahedra and triangular prisms are colored orange and blue, respectively. The difference between the EAS-predicted and the DFT-calculated interatomic distances is denoted by Δ here.

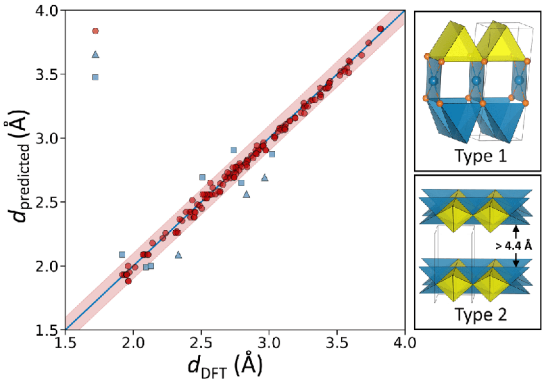

Figure 5 (Color online) Predicted interatomic distances for binary compounds between IA/IIA and VIA/VIIA elements using EAS model, in comparison with the DFT results. For most of the compounds, the absolute difference (|Δ|) between the EAS-predicted and the DFT-calculated results is below 0.1 Å. Compounds with Type 1 or Type 2 structures tend to produce large deviation.

quently highlighted in the literature of HS and SS models [18,23].

The validity of EAS model in predicting interatomic distances is further demonstrated in Figure 5 for nearly all binary compounds between IA/IIA and VIA/VIIA elements that are composed of structural units with CN of 4, 6 or 8. A total of 148 bond length data are gathered from latest inorganic crystal structure databases mentioned above (structural data are listed in Table S2). Using the DFT results of this data set as a reference, the majority of the EAS-predicted interatomic distances lie within an error band of ± 0.1 Å (most of them less than ± 0.05 Å), a value that is even smaller than the average deviation calculated from HS model (0.11 Å). To enable a comparison, we also modify the HS model (HS-modified) by fixing the radii to the HS values during the fitting procedure of parameters $k^{(4)}$, $k^{(6)}$ and $k^{(8)}$. The average deviation of interatomic distances calculated from HS-modified model is 0.056 Å, higher than the EAS model. Several compounds with regular structures (Figure S3) exhibit large deviation that undermines the predictability of the former model. In this respect, it is necessary to introduce a new set of radii other than the HS radii such that the interatomic distances can be precisely predicted, and this is what the EAS model can achieve.

The exceptions to the general validity of EAS model come only for two specific structures shown in Figure 5, here denoted by Type 1 and Type 2 structures. In Type 1 structure which appears in MgO, MgS and MgSe (Figure S4(a)), structural units in the form of planar MgO_4 exhibit an extreme case of distortion with shortened O-O bonds that in turn repel the next-nearest-neighbor Mg ions. This would result in longer Mg-O bond lengths than those anticipated by EAS model. On the other hand, in Type 2 structure which appears in MgO, MgSe and MgTe (Figure S4(b)), ions in MgO_4 and MgO_6 structural units are distributed in a layered, planar pattern, with the layers stacking via the weak van der Waals bonds. Such a pattern would inevitably interfere with the ionic bonding character within a layer, thus producing large fluctuations in interatomic distances. Consequently, both Type 1 and Type 2 structures can be considered abnormal in ionic crystals. Indeed, given that only normal ionic crystals are involved in the fitting procedure, it is comprehensible that the comparison between the predicted and the DFT-calculated results would filter out the abnormal structures in the data set. Another issue that warrants attention is that such abnormality prevails in complex compounds which are consisted of multiple elements, such as ternary ionic compounds that generally contain structural units with CN of 3, 5 and 7. These complex structures and their peculiar coordination environment will result in large deviation in interatomic distances even in a single structural unit. This factor prevents us from analyzing the crystals built of those structural units. The above results also lead to a method of fitting-predicting from large data sets for detecting the abnormal structures that may correspond to unusual properties, which can probably give rise to fruitful advance in our knowledge of ionic crystals.

5 Conclusions

In summary, an effective atomic size model is proposed for estimating the ionic radii and predicting the interatomic distances in novel ionic materials. A set of EAS radii including most of the Group IA, IIA, VIA and VIIA elements is summarized with their corresponding k values used in the EAS model. We demonstrate how by defining the role of neighboring atoms in calculating the interatomic distances it is possible to achieve better agreement between the predicted

and the real interatomic distances than the previous models. Furthermore, it is shown preliminarily that moderate distortion and symmetry breaking of the structural units may exert little influence on the relationship between ionic radii and interatomic distances, while the coordination numbers of the ions appear as a determinant. Moreover, the robustness and accuracy in predicting interatomic distances using EAS model are illustrated by a large data set including nearly all binary ionic compounds from different latest databases. We believe that the effective atomic size in structure unit of ionic crystals can be a descriptor of "Material Genes" and the EAS model can serve as a universal basis for predicting the arrangements of atoms when carrying out high-throughput searches for materials with new structures.

This work was supported by the National Key R&D Program of China (Grant No. 2016YFB0700600), the Shenzhen Science and Technology Research (Grant No. ZDSYS201707281026184), and the Guangdong Key-Lab Project (Grant No. 2017B0303010130).

Supporting Information

The supporting information is available online at tech.scichina.com and link.springer.com. The supporting materials are published as submitted, without typesetting or editing. The responsibility for scientific accuracy and content remains entirely with the authors.

1 Shi S Q, Gao J, Liu Y, et al. Multi-scale computation methods: Their applications in lithium-ion battery research and development. Chin Phys B, 2016, 25: 018212
2 Liu Y, Zhao T, Ju W, et al. Materials discovery and design using machine learning. J Materiomics, 2017, 3: 159–177
3 Bragg W L. The arrangement of atoms in crystals. Philos Mag, 1920, 40: 169–189
4 Goldschmidt V M. Die gesetze der krystallochemie. Naturwissenschaften, 1926, 14: 477–485
5 Pauling L. The sizes of ions and the structure of ionic crystals. J Am Chem Soc, 1927, 49: 765–790
6 Slater J C. Atomic shielding constants. Phys Rev, 1930, 36: 57–64
7 Pauling L. The nature of the chemical bond. Application of results obtained from the quantum mechanics and from a theory of paramagnetic susceptibility to the structure of molecules. J Am Chem Soc, 1931, 53: 1367–1400
8 Zachariasen W H. A set of empirical crystal radii for ions with inert gas configuration. Z Für Krist-Cryst Mater, 2015, 80: 137–153
9 Ahrens L H. The use of ionization potentials Part 1. Ionic radii of the elements. GeoChim CosmoChim Acta, 1952, 2: 155–169
10 Slater J C. Atomic radii in crystals. J Chem Phys, 1964, 41: 3199–3204
11 Shannon R D, Prewitt C T. Effective ionic radii in oxides and fluorides. Acta Crystlogr B Struct Sci, 1969, 25: 925–946
12 Shannon R D. Revised effective ionic radii and systematic studies of interatomic distances in halides and chalcogenides. Acta Cryst A, 1976, 32: 751–767
13 Schweinfest R, Paxton A T, Finnis M W. Bismuth embrittlement of copper is an atomic size effect. Nature, 2004, 432: 1008–1011
14 Greaves G N, Gurman S J, Catlow C R A, et al. A structural basis for ionic diffusion in oxide glasses. Philos Mag A, 2006, 64: 1059–1072
15 Bishop S R, Perry N H, Marrocchelli D, et al. Electro-Chemo-Mechanics of Solids. Cambridge: Springer International Publishing, 2017
16 Shuttleworth R. The surface tension of solids. Proc Phys Soc A, 1950, 63: 444–457
17 Cordero B, Gómez V, Platero-Prats A E, et al. Covalent radii revisited. Dalton Trans, 2008, 40: 2832–2838
18 Pauling L. The Nature of the Chemical Bond. Ithaca: Cornell University Press, 1960. 260
19 Gibbs G V, Ross N L, Cox D F, et al. Bonded radii and the contraction of the electron density of the oxygen atom by bonded interactions. J Phys Chem A, 2013, 117: 1632–1640
20 Holbrook J B, Khaled F M, Smith B C. Soft-sphere ionic radii for Group 1 and Group 2 metal halides and ammonium halides. J Chem Soc Dalton Trans, 1978, 12: 1631–1634
21 Collin R J, Smith B C. Ionic radii for Group 1 halide crystals and ion-pairs. Dalton Trans, 2005, 4: 702–705
22 Lang P F, Smith B C. Ionic radii for Group 1 and Group 2 halide, hydride, fluoride, oxide, sulfide, selenide and telluride crystals. Dalton Trans, 2010, 39: 7786–7791
23 Lang P F, Smith B C. Electronegativity effects and single covalent bond lengths of molecules in the gas phase. Dalton Trans, 2014, 43: 8016–8025
24 Jain A, Ong S P, Hautier G, et al. Commentary: The Materials Project: A materials genome approach to accelerating materials innovation. APL Mater, 2013, 1: 011002
25 Jain A, Hautier G, Moore C J, et al. A high-throughput infrastructure for density functional theory calculations. Comput Mater Sci, 2011, 50: 2295–2310
26 Belsky A, Hellenbrandt M, Karen V L, et al. New developments in the inorganic crystal structure database (ICSD): Accessibility in support of materials research and design. Acta Cryst Sect A Found Cryst, 2002, 58: 364–369
27 Bergerhoff G, Hundt R, Sievers R, et al. The inorganic crystal structure data base. J Chem Inf Model, 1983, 23: 66–69
28 Gražulis S, Daškevič A, Merkys A, et al. Crystallography open database (COD): An open-access collection of crystal structures and platform for world-wide collaboration. Nucleic Acids Res, 2012, 40: D420–D427
29 Cotton F A, Wilkinson G. Advanced Inorganic Chemistry. New York: Wiley, 1988. 6
30 Pauling L. Soft-sphere ionic radii for alkali and halogenide ions. J Chem Soc Dalton Trans, 1980, 645–645
31 Batsanov S S. The atomic radii of the elements. Russ J Inorg Chem, 1991, 36: 1694–1706
32 Kresse G, Hafner J. *Ab initio* molecular dynamics for liquid metals. Phys Rev B, 1993, 47: 558–561
33 Kresse G, Furthmüller J. Efficient iterative schemes for *ab initio* total-energy calculations using a plane-wave basis set. Phys Rev B, 1996, 54: 11169–11186
34 Kohn W, Sham L J. Self-consistent equations including exchange and correlation effects. Phys Rev, 1965, 140: A1133–A1138
35 Khein A, Singh D J, Umrigar C J. All-electron study of gradient corrections to the local-density functional in metallic systems. Phys Rev B, 1995, 51: 4105–4109
36 dal Corso A, Pasquarello A, Baldereschi A, et al. Generalized-gradient approximations to density-functional theory: A comparative study for atoms and solids. Phys Rev B, 1996, 53: 1180–1185
37 Staroverov V N, Scuseria G E, Tao J, et al. Tests of a ladder of density functionals for bulk solids and surfaces. Phys Rev B, 2004, 69: 075102
38 Haas P, Tran F, Blaha P. Calculation of the lattice constant of solids with semilocal functionals. Phys Rev B, 2009, 79: 085104